THE JOURNAL OF BIOLOGICAL CHEMISTRY

Vol. 271, No. 16, Issue of April 19, pp. 9535–9545, 1996
Printed in U.S.A.

Cardiotrophin-1 Activates a Distinct Form of Cardiac Muscle Cell Hypertrophy

ASSEMBLY OF SARCOMERIC UNITS IN SERIES VIA gp130/LEUKEMIA INHIBITORY FACTOR RECEPTOR-DEPENDENT PATHWAYS*

(Received for publication, July 26, 1995, and in revised form, February 7, 1996)

Kai C. Wollert‡§, Tetsuya Taga¶, Mikiyoshi Saito¶, Masashi Narazaki¶, Tadamitsu Kishimoto‖, Christopher C. Glembotski, Ann B. Vernallis‡‡, John K. Heath‡‡, Diane Pennica§§, William I. Wood§§, and Kenneth R. Chien‡¶¶**

*From the ‡Department of Medicine, Center for Molecular Genetics, and the American Heart Association-Bugher Foundation Center for Molecular Biology, University of California, San Diego, School of Medicine, La Jolla, California 92093, ¶Institute for Molecular and Cellular Biology, Osaka University, Osaka, Japan, ‖Department of Medicine III, Osaka University Medical School, Osaka, Japan, **Department of Molecular Biology, San Diego State University, San Diego, California 92182, ‡‡Department of Biochemistry, University of Oxford, Oxford, United Kingdom, and the §§Department of Molecular Biology Genentech, Inc., South San Francisco, California 94080*

Cardiotrophin-1 (CT-1) was recently isolated by expression cloning based on its ability to induce an increase in cell size in neonatal rat ventricular cardiomyocytes. Sequence similarity data suggested that CT-1 is a novel member of a family of structurally related cytokines sharing the receptor component gp130. The present study documents that gp130 is required for CT-1 signaling in cardiomyocytes, by demonstrating that a monoclonal anti-gp130 antibody completely inhibits c-*fos* induction by CT-1. Similarly, a leukemia inhibitory factor receptor subunit β (LIFRβ) antagonist effectively blocks the CT-1 induction of c-*fos*, indicating a requirement for LIFRβ in the hypertrophic response, as well. Upon stimulation with CT-1, both gp130 and the LIFRβ are tyrosine-phosphorylated, providing further evidence that CT-1 signals through the gp130/LIFRβ heterodimer in cardiomyocytes. CT-1 induces a hypertrophic response in cardiomyocytes that is distinct from the phenotype seen after α-adrenergic stimulation, both with regard to cell morphology and gene expression pattern. Stimulation with CT-1 results in an increase in cardiac cell size that is characterized by an increase in cell length but no significant change in cell width. Confocal laser microscopy of CT-1 stimulated cells reveals the assembly of sarcomeric units in series rather than in parallel, as seen after α-adrenergic stimulation. CT-1 induces a distinct pattern of immediate early genes, and up-regulates the atrial natriuretic factor (ANF) gene, but does not affect skeletal α-actin or myosin light chain-2v expression. As evidenced by nuclear run-on transcription assays, both CT-1 and α-adrenergic stimulation lead to an increase in ANF gene transcription. Transient transfection analyses document that, in contrast to α-adrenergic stimulation, the CT-1 responsive *cis*-regulatory elements are located outside of the proximal 3 kilobase pairs of the ANF 5′-flanking region. These studies indicate that CT-1 can activate a distinct form of myocardial cell hypertrophy, characterized by the promotion of sarcomere assembly in series, via gp130/LIFRβ-dependent signaling pathways.

Hypertrophy is one of the most important compensatory responses of the myocardium, as it is critical for the maintenance of normal cardiac function in response to pressure overload in the setting of hypertension or volume overload during valvular insufficiency. However, the mechanical stimuli of pressure *versus* volume overload produce distinct cardiac muscle phenotypes, with the former resulting in a concentric pattern of hypertrophy, and the latter promoting an eccentric form of hypertrophy with cardiac chamber dilation. On a single cell level, cardiac myocytes isolated from concentric hypertrophic hearts display an increase in cell diameter with the addition of new myofibrils in parallel (1, 2), while myocytes derived from dilated hearts exhibit an increase in cell length, reflecting the addition of new sarcomeric units in series (3, 4). These distinct morphological phenotypes are associated with different effects on global cardiac function. Chronic volume overload hypertrophy can result in an irreversible loss of cardiac function, while pressure overload hypertrophy is usually associated with the preservation of contractile function, and can often be reversible. While both forms of hypertrophy can lead to the induction of the atrial natriuretic factor gene, distinct molecular phenotypes have also recently been observed (5). Although it has long been accepted that there are distinct morphologic forms of hypertrophy in the setting of pressure or volume overload, the signaling pathways which mediate these distinct cardiac phenotypes remain unclear. One of the critical questions is whether divergent signaling pathways are responsible for the activation of these distinct forms of hypertrophy that display clear differences with respect to cell morphology, physiology, and the induction of molecular markers.

Our current insight into the mechanisms controlling cardiomyocyte hypertrophy has primarily been obtained from an *in vitro* model employing neonatal rat ventricular myocytes. A number of growth factors signaling through G-protein coupled receptors, including α-adrenergic agonists (6–11), endothelin 1 (12, 13), and angiotensin II (14), promote a hypertrophic response in this *in vitro* system. Following activation of the

* This work was supported in part by National Institutes of Health, NHLBI Grants 1 RO1 HL51549, PO1 HL46345, HL53773, and AHA 91–022170 (to K. R. C.), and by a fellowship from the Deutsche Forschungsgemeinschaft (Wo 552/1-1) (to K. C. W.). The costs of publication of this article were defrayed in part by the payment of page charges. This article must therefore be hereby marked "*advertisement*" in accordance with 18 U.S.C. Section 1734 solely to indicate this fact.

§ Present address: Universität Freiburg, Medizinische Klinik, Abt. Kardiologie, Hugstetterstr. 55, 79106 Freiburg, Germany.

¶¶ To whom correspondence should be addressed: Dept. of Medicine and Center for Molecular Genetics, University of California, San Diego, 9500 Gilman Dr., La Jolla, CA 92093-0613. Tel.: 619-534-6835; Fax: 619-534-8081.

G-protein-dependent pathways, cardiomyocytes display a uniform enlargement of cell size, with increases in cell width and length, resulting from the assembly of new myofibrils in parallel (12, 15, 16). *ras*-dependent pathways appear to be both necessary and sufficient to activate the hypertrophic response following α-adrenergic stimulation in the *in vitro* model system (17), and a recent study in transgenic mice documented that the overexpression of a constitutively active *ras* protein in the ventricular chambers results in a concentric form of cardiac hypertrophy (18). Taken together, these studies indicate that G-protein coupled receptors and *ras*-dependent pathways activate a form of cardiac hypertrophy that resembles the hypertrophy seen in the setting of pressure overload. The question arises as to whether divergent signaling pathways would mediate a volume overload like hypertrophic phenotype, characterized by sarcomere assembly in series and myocyte enlargement primarily due to an increase in cell length *versus* width.

By coupling expression cloning to a miniaturized version of the *in vitro* hypertrophy assay, we have recently isolated a novel 21.5-kDa protein that induces an increase in cell size and atrial natriuretic factor (ANF)[1] release in cardiomyocytes (19). The protein was designated cardiotrophin-1 (CT-1). Sequence similarity data and structural considerations suggest that CT-1 is a new member of a family of structurally related cytokines including interleukin (IL)-6 and IL-11, leukemia-inhibitory factor (LIF), ciliary neurotrophic factor (CNTF), and oncostatin M (OSM). The receptors of this cytokine family are multimeric and share the class-specific transmembrane signal transducing component gp130 (20–23). Signaling is triggered through the homodimerization of gp130 (24), or the heterodimerization of gp130 with a related transmembrane signal transducer, the LIF receptor subunit β (LIFRβ (25, 26). The gp130/LIFRβ heterodimer constitutes the functional bipartite LIF receptor complex (22, 27). Other members of this cytokine family first bind to a private receptor component and subsequently induce gp130 dimerization. For example, IL-6 binds to the receptor component IL-6R, and the IL-6·IL-6R complex then induces the homodimerization of gp130 (28, 29); CNTF binds to the receptor component CNTFRα and induces gp130/LIFRβ heterodimerization (26, 30, 31). Consequently, the expression pattern of the various receptor components defines the spectrum of action of different members of the gp130 cytokine family.

The cloning of CT-1 based on its ability to induce an increase in cell size in cardiomyocyte culture (19) suggested that gp130-dependent signaling pathways may be coupled to cardiomyocyte hypertrophy. In the present study we define the receptor system used by CT-1 in cardiomyocytes, and we examine the effects of CT-1 and two other members of the IL-6 cytokine family, LIF and CNTF, on morphological and molecular features defining a hypertrophic response in cultured cardiomyocytes. By using a monoclonal anti-gp130 antibody and a LIFRβ antagonist, we establish that both gp130 and LIFRβ are required for CT-1 signaling in cardiomyocytes. Immunoprecipitation and immunoblotting data show that CT-1 induces the tyrosine phosphorylation of gp130 and a higher molecular weight protein, corresponding in size to LIFRβ. Using confocal laser microscopy of cells stained for both thick and thin filament markers, our studies further indicate that gp130/LIFRβ-dependent signaling pathways induce a hypertrophic phenotype in cardiomyocytes that is distinct from the response seen after α-adrenergic stimulation, and that shows resemblance to volume overload cardiac hypertrophy both with regard to cell morphology and gene expression pattern.

EXPERIMENTAL PROCEDURES

Murine LIF was produced at Genentech, Inc. Murine LIF was used throughout the study, except for the experiment employing the LIFRβ antagonist (hLIF-04), in which both murine LIF and human LIF were used. Rat CNTF and human IL-6 were purchased from Boehringer Mannheim and from Genzyme, respectively. Human sIL-6R was prepared as outlined previously (21). The α-adrenergic agonist phenylephrine (PE) was obtained from Sigma.

Expression and Purification of the CT-1 Fusion Protein—The reading frame of murine CT-1 was cloned C-terminal to the sequence encoding the herpes simplex virus glycoprotein D followed by a factor Xa cleavage site. Following expression in 293 cells and cleavage of the herpes simplex virus secretion signal sequence, the CT-1 fusion protein contained a 34-amino acid N-terminal extension followed by the CT-1 sequence (19). The CT-1 fusion protein was purified from conditioned medium with a herpes simplex virus glycoprotein D-specific monoclonal antibody and quantified by a colorimetric assay (Bio-Rad).

LIFRβ Antagonist hLIF-04—The LIFRβ antagonist hLIF-04 was used to assess the requirement of the LIFRβ for CT-1 signaling. Human LIF (hLIF) and the hLIF mutant, hLIF-04, were expressed as glutathione *S*-transferase fusion proteins, as described previously (32). hLIF-04 contains three amino acid substitutions (Q25A, S28A, and Q32A), within the A-helix of the hLIF molecule, resulting in a selective disruption of the gp130 binding site, but no impairment in LIFRβ binding. A detailed characterization of the LIFRβ antagonist hLIF-04 will be presented elsewhere.[2]

Cell Culture—Hearts from 1–3-day-old Sprague-Dawley rats were removed, the ventricles were pooled, and the ventricular cells were dispersed by digestion with collagenase II (Worthington) and pancreatin (Life Technologies, Inc.). The cell suspension was purified by centrifugation through a discontinuous Percoll gradient to obtain myocardial cell cultures with >95% myocytes, as assessed by immunofluorescence with an anti-TrpE/MLC-2v antiserum (12, 33). The cardiomyocytes were plated at a density of $5–6 \times 10^4$ cells/cm^2 in Dulbecco's modified Eagle's medium (DMEM)/medium 199 (4:1) supplemented with 10% horse serum, 5% fetal bovine serum, glutamine and antibiotics (plating medium), and allowed to attach overnight. The cells were then washed twice with DMEM/medium 199 and further incubated in DMEM/medium 199 supplemented with glutamine and antibiotics (maintenance medium) in the presence or absence of various agents. Neonatal *mouse* ventricular myocytes were isolated from 1–4-day-old NIH Swiss mice, following the protocol outlined above. One litter (8–12 pups) yielded $\sim 5 \times 10^5$ cells. Approximately 95% of the cells displayed spontaneous contractile activity in culture.

Immunoprecipitation and Immunoblotting—Cardiomyocytes were stimulated with various agents and solubilized with ice cold lysis buffer (0.5% Nonidet P-40, 150 mM NaCl, 10 mM Tris-HCl, pH 8.0, 5 mM EDTA, 2 mM sodium vanadate, 1 mM *p*-amidinophenylmethanesulfonyl fluoride (Sigma), 5 μg/ml aprotinin). Clear lysates were obtained by centrifugation and immunoprecipitated with a polyclonal rabbit anti-gp130 cytoplasmic peptide antibody (34). Immunoprecipitates (protein A-Sepharose, Pharmacia Biotech Inc.) were subjected to SDS-PAGE under reducing conditions and immunoblotted with an anti-phosphotyrosine antibody (4G10, Upstate Biotechnology), employing an enhanced chemiluminescence detection system (Amersham Corp.). For the detection of protein tyrosine phosphorylation, the cell lysates were analyzed directly by SDS-PAGE and immunoblotting with 4G10.

Immunofluorescence Techniques and Morphometric Analysis—Cardiomyocytes were plated in Lab-Tek plastic chamber slides (Nunc), precoated with 4 μg/cm^2 laminin (Sigma), and incubated in the presence or absence of various agents. After 48 h, the cells were rinsed with phosphate-buffered saline, fixed in 4% paraformaldehyde, and permeabilized with 0.3% Triton X-100. Following three phosphate-buffered saline washes, the chamber slides were incubated in 3% bovine serum albumin for 10 min to block nonspecific sites. Subsequently, the cells

[1] The abbreviations used are: ANF, atrial natriuretic factor; CT-1, cardiotrophin-1; LIF, leukemia inhibitory factor; hLIF, human LIF; IL, interleukin; CNTF, ciliary neurotrophic factor; CNTFR, CNTF receptor; OSM, oncostatin M; PE, phenylephrine; (s)IL-6R, (soluble) IL-6 receptor; LIFRβ, LIF receptor subunit β; MLC-2v, ventricular myosin light chain-2; βMHC, β myosin heavy chain; GAPDH, glyceraldehyde-3-phosphate dehydrogenase; DMEM, Dulbecco's modified Eagle's medium; Tricine, *N*-[2-hydroxy-1,1-bis(hydroxymethyl)ethyl]glycine; I.E., immediate early; PAGE, polyacrylamide gel electrophoresis; RSV, Rous sarcoma virus; bp, base pair(s); kb, kilobase pair(s).

[2] K. R. Hudson, A. B. Vernallis, and J. K. Heath, manuscript submitted for publication.

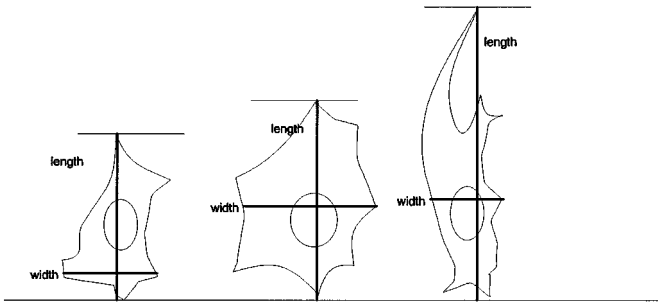

FIG. 1. **Definition of morphometric parameters.** Cell length was defined as the maximum longitudinal extension of individual cells. Maximum cell width was measured perpendicular to the axis defining cell length.

were dual-stained for 1 h in 3% bovine serum albumin with 1) a polyclonal anti-TrpE/MLC-2v antiserum from rabbit (12), combined with a monoclonal mouse anti-rat ANF antibody (35, 36), or 2) a monoclonal mouse anti-human β myosin heavy chain (βMHC) antibody (37), combined with rhodamine phalloidine (Molecular Probes). Following four phosphate-buffered saline washes, the slides were blocked with 5% normal donkey serum for 10 min, incubated for 1 h in 5% normal donkey serum using a Texas Red-conjugated donkey anti-rabbit IgG and a fluorescein isothiocyanate-conjugated donkey anti-mouse IgG as secondary antibodies (Jackson Laboratories), and finally mounted on glass coverslips. Cardiomyocytes stained against MLC-2v and ANF were viewed by fluorescence microscopy. Cell size was estimated by measuring the area to which individual MLC-2v-positive cells attached (planimetry), cell length and width were determined as outlined in Fig. 1, and the percentage of MLC-2v positive cells that displayed perinuclear staining for immunoreactive ANF was calculated. Cardiomyocytes stained against βMHC and F-actin (rhodamine phalloidine) were analyzed by confocal laser microscopy using a 60 × oil immersion objective. Images of cardiomyocytes stained against βMHC were used to determine the effect of various agonists on the average sarcomere length.

ANF Radioimmunoassay—The concentration of immunoreactive ANF in cell culture supernatants was determined by radioimmunoassay, using the monoclonal mouse anti-rat ANF antibody with synthetic ANF-(99-126) as the standard and ^{125}I-ANF-(99-126) (Amersham) as the trace (35).

Isolation and Hybridization of RNA—Total cellular RNA was isolated by a modification of the acid guanidium/thiocyanate phenol/chloroform extraction method (38) using the RNA STAT 60 RNA isolation reagent (Tel-Test "B"). RNA was size-fractionated by formaldehyde agarose gel electrophoresis, transferred to nylon filters (Magna NT) by overnight capillary blotting, and hybridized with cDNA probes labeled with [α-^{32}P]dCTP by random priming (Life Technologies, Inc.). The filters were washed under stringent conditions and exposed to x-ray film (Kodak X-Omat AR). Signal intensities were determined by densitometry (UltroScan XL, Pharmacia). The following cDNA probes were used: mouse c-*fos* (1.2-kb fragment) (39), mouse *egr-1* (zif/268) (1.7-kb fragment (40), human c-*myc* (1.6-kb fragment, a generous gift of Dr. J. Feramisco), mouse c-*jun* (2.6-kb fragment) (41), mouse *jun*-B (1.90-kb fragment) (42), mouse *tis11* (1.0-kb fragment, a generous gift of Dr. H. R. Herschman) (43), rat prepro-ANF (0.6 kb of coding region) (44), rat skeletal α-actin (0.2 kb of a 3′-untranslated region generated by reverse transcriptase-polymerase chain reaction from skeletal muscle poly(A)$^+$ RNA) (45) and rat MLC-2v (0.6 kb of coding region) (46). Human glyceraldehyde-3-phosphate dehydrogenase (GAPDH) (1.2-kb fragment) (47) and mouse 28s (5-kb fragment) cDNA probes were used to control for loading and transfer efficiency.

Nuclear Run-on Transcription Assay—Run-on transcription assays were performed as described previously (48). Cardiomyocytes were lysed in ice-cold Nonidet P-40 buffer (10 mM Tris-HCl, pH 7.5, 10 mM NaCl, 3 mM $MgCl_2$, 0.5% Nonidet P-40) and further disrupted by 10 gentle strokes with a loose pestle in a Dounce homogenizer. The nuclei were recovered by centrifugation. The supernatants (representing the cytosolic fractions) were saved, and vanadylribonucleoside complexes (Life Technologies, Inc.) were added to inhibit RNase activity. Total RNA was isolated from the cytosolic fractions and subjected to Northern blot analysis using prepro-ANF, GAPDH, and 28s cDNA probes. The nuclei were washed once in Nonidet P-40 buffer, resuspended in 100 μl of storage solution (50% glycerol, 50 mM HEPES, pH 7.4, 5 mM $MgCl_2$, 0.1 mM EDTA, 5 mM dithiothreitol), and stored at −80 °C. On the day of the assay, the nuclei were thawed, 27.5 μl of run-on buffer (25 mM Tris-HCl, pH 7.5, 12.5 mM $MgCl_2$, 750 mM KCl, 25 mM dithiothreitol, 1.25 mM of ATP, GTP, and CTP), 6 μl (62.5 μCi) of [α-^{32}P]UTP, and 1 μl of RNasin (Promega) were added, and the nuclei were incubated at 30 °C for 30 min. Following DNA and protein digestion (RQ-1 DNase 1, Promega; proteinase K, Life Technologies, Inc.), the ^{32}P-labeled RNA was extracted once with phenol/chloroform, ethanol-precipitated, and purified over a RNase-free Sephadex G50 column (Boehringer Mannheim). The total amount of ^{32}P-labeled RNA recovered from each reaction was determined by liquid scintillation counting (Beckman). Five micrograms of linearized, alkali-denatured pBluescript (Stratagene), pBluescript harboring the rat prepro-ANF cDNA (44), and pBluescript harboring the human GAPDH cDNA (47) were spotted onto nylon filters in advance. The filters were prehybridized for 1 h in 56.25% formamide, 0.25 M sodium phosphate, pH 7.2, 0.25 M NaCl, 1 mM EDTA, 7% SDS. An equal number of counts from each run-on reaction were added to the prehybridization solution, and hybridizations were carried out for 48 h at 42 °C. Finally, the filters were washed under stringent conditions and exposed to x-ray film. The amount of ANF and GAPDH-specific hybridization was determined by densitometry. No hybridization to the empty pBluescript control was detectable (data not shown).

Plasmid Constructs—pANF(−3003)Luc5′, an ANF-luciferase reporter construct composed of the most proximal 3003 bp of the rat ANF gene 5′-flanking region inserted into the promoterless firefly luciferase reporter plasmid pSVOALuc5′ was used to assess the CT-1-, LIF-, CNTF-, and PE-induced activity of the rat ANF promoter (11). pRSV-Luc5′, a RSV-luciferase reporter construct, and pSVOALuc5′ served as positive and negative controls, respectively (49). To correct for transfection efficiency, cardiomyocytes were cotransfected with pON249, a β-galactosidase expression vector under the control of the human cytomegalovirus promoter (50).

Transfection and Luciferase/β-Galactosidase Assays—Cells were plated in 3.5-cm dishes in duplicate, allowed to attach overnight, and switched to maintenance medium supplemented with 4% horse serum. Two hours later, the cells were cotransfected with 2.75 μg of either pANF(−3003)Luc5′, pRSVLuc5′, or pSVOALuc5′, and 0.75 μg of pON249 using the calcium phosphate method as described by Chen and Okayama (51). After 18–20 h, the cells were washed twice to remove the fine layer of calcium precipitate and incubated in maintenance medium in the presence or absence of various agents. At different time points, the cells were washed twice with ice-cold phosphate-buffered saline and were lysed for 30 min on ice in 100 μl of lysis buffer (0.1 M KH_2PO_4, pH 7.9, 0.5% Triton X-100, 1 mM dithiothreitol). Luciferase activities were determined in duplicate samples from each plate; 20 μl of cell lysate were combined with 100 μl of luciferase assay buffer (100 mM Tricine, pH 7.8, 10 mM $MgSO_4$, 2 mM EDTA, 2 mM ATP, 1 mM dithiothreitol, 73 μM β-luciferin), and luciferase activities were measured using a Monolight 401 luminometer (Analytical Luminescence Laboratory). β-Galactosidase activities were determined in duplicate samples from each plate; 20 μl of cell lysate were added to 250 μl of β-galactosidase assay buffer (0.1 M sodium phosphate, pH 7.3, 1.2 mM $MgCl_2$, 60 mM β-mercaptoethanol, 1.8 mM chlorophenol red-β-D-galactopyranoside (Boehringer Mannheim)), and incubated at 37 °C for 15 min. β-Galactosidase activities were obtained by measuring OD at 574 nm, using lysis buffer as a blank.

Statistical Analysis—Data are presented as means ± S.E. p values were determined using one-way analysis of variance.

RESULTS

Induction of a Distinct Pattern of Immediate Early Genes following CT-1 versus α-Adrenergic Stimulation of Cultured Myocardial Cells—The induction of immediate early (I.E.) genes precedes the late phenotypic changes in cardiomyocytes following the stimulation of G-protein-coupled receptors *in vitro* (12–15) and cardiac hypertrophy *in vivo* (52, 53). We therefore determined whether stimulation of cardiomyocytes with CT-1, LIF, or CNTF would induce I.E. gene expression (Fig. 2). Stimulation with CT-1 resulted in the rapid and transient induction of a panel of I.E. genes, including c-*fos*, *egr-1*, c-*myc*, c-*jun*, *jun*-B, and *tis11*. The pattern of I.E. gene expression in response to stimulation with LIF was virtually indistinguishable from the pattern induced by CT-1. CNTF displayed a relatively weak induction of the same panel of I.E. genes as did CT-1 and LIF. As compared to stimulation with PE, CT-1, and LIF induced >10 fold higher levels of c-*myc* and *tis11*.

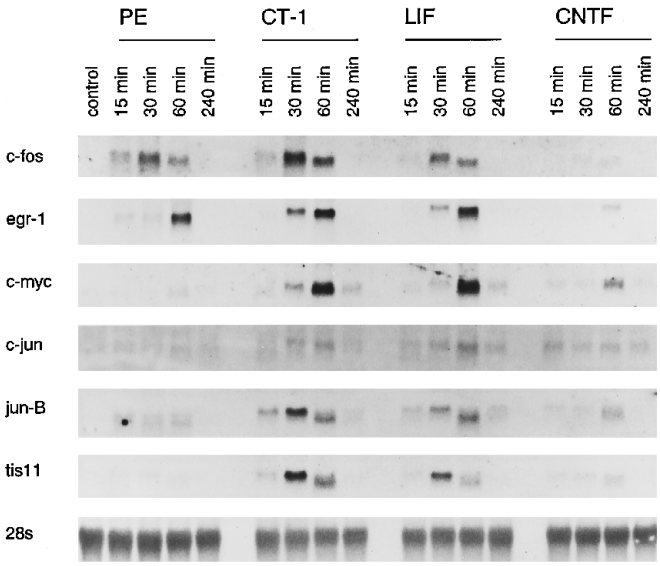

FIG. 2. **Immediate early gene induction.** Neonatal rat ventricular cardiomyocytes were plated into 15-cm dishes and serum-starved for 18 h. Thereafter, control cells were harvested; the remaining cells were stimulated with PE (100 μM), CT-1, LIF, or CNTF (1 nM each), for the indicated times. Total RNA was isolated and subjected to Northern blot analysis (10 μg/lane). The following probes were used: c-*fos*, *egr-1*, c-*myc*, c-*jun*, *jun*-B, *tis11*, and 28s. Data from one experiment are presented. One additional experiment yielded comparable results.

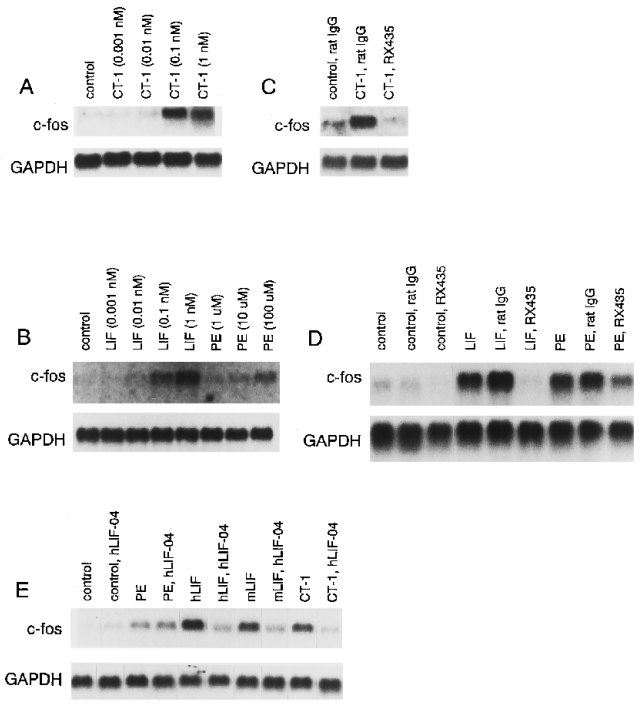

FIG. 3. **Effects of an anti-gp130 antibody and a LIFRβ antagonist on the c-*fos* induction by CT-1, LIF, and phenylephrine.** Neonatal mouse ventricular cardiomyocytes were plated into 3.5-cm dishes and serum-starved for 18 h. Thereafter, the cells were stimulated for 45 min with various concentrations of CT-1, LIF, or PE (*Panels A* and *B*). In a second set of experiments, cells were incubated with a monoclonal rat anti-mouse gp130 antibody (RX435, 20 μg/ml) or immunopurified rat IgG (20 μg/ml) prior to CT-1 (0.1 nM) stimulation (*Panel C*), and LIF (0.1 nM) or PE (100 μM) stimulation (*Panel D*). In a third experiment (*Panel E*), cells were incubated with a LIFRβ antagonist (hLIF-04, 0.5 nM), prior to stimulation with PE (100 μM), human LIF (*hLIF*), murine LIF (*mLIF*), and CT-1 (0.1 nM each). Total RNA was isolated and subjected to Northern blot analysis (2 μg/lane). Equal loading and transfer conditions were confirmed by GAPDH and 28s (not shown) hybridization.

Involvement of gp130 and LIFRβ in CT-1 Induction of c-fos—Previous studies have employed blocking antibodies directed against gp130 to demonstrate that IL-6, LIF, OSM, CNTF, and IL-11 utilize the common receptor component gp130 (21–23). Sequence similarity data, as well as structural considerations, suggest that CT-1 might be a new member of this cytokine family, and might therefore share the receptor component gp130 (19). To directly test this hypothesis, we examined the effect of an anti-gp130 antibody on the CT-1 induction of c-*fos* in cardiomyocytes. A monoclonal anti-gp130 antibody (RX435) was generated by immunizing rats with recombinant murine gp130.[3] RX435 specifically blocks the action of LIF, IL-6, IL-11, and OSM on mouse myeloid leukemic M1 cells[3] and inhibits the binding of CT-1 to M1 cells (54). Since RX435 does not cross-react with rat gp130, we used neonatal mouse cardiomyocytes in this set of experiments. Similar to the rat system, murine cardiomyocytes responded to stimulation with CT-1, LIF, and PE with an induction of immediate early genes and typical morphology changes. However, CT-1, LIF, and PE did not induce ANF gene expression in murine cardiomyocytes (data not shown). This might relate to the fact that in mice, in sharp contrast to rats, the ventricular expression of ANF is not down-regulated after birth, but instead remains at high levels from embryogenesis through adulthood (55). We first examined the effects of different concentrations of CT-1, LIF and PE on the induction of c-*fos* in murine cardiomyocytes. CT-1, LIF, and PE induced c-*fos* expression in a dose-dependent manner (Fig. 3, *A* and *B*). In subsequent experiments, cardiomyocytes were incubated for 1 h with RX435 or, as a control, with immunopurified rat IgG prior to stimulation with CT-1, LIF, or PE. RX435 was used at a concentration that has previously been shown to inhibit ~80% of CT-1 (0.12 nM) binding to murine M1 cells (54). CT-1, LIF, and PE were used at concentrations that resulted in an approximately 4–5-fold induction of c-*fos* expression. As shown in Fig. 3, *C* and *D*, RX435 completely abolished the induction of c-*fos* by CT-1 and LIF. By contrast, the c-*fos* induction by PE was not abolished by RX435 (although somewhat suppressed), confirming the specificity of the antibody (Fig. 3*D*).

To determine whether LIFRβ is required for CT-1 signaling, we studied the effect of a LIFRβ antagonist, hLIF-04, on c-*fos* induction by CT-1. hLIF-04 was generated by introducing three amino acid substitutions in the human LIF molecule, thereby abrogating the gp130 binding site. hLIF-04 has been shown to antagonize the action of hLIF in a Ba/F3 cell line, stably transfected with human gp130 and LIFRβ (see "Experimental Procedures"). As shown in Fig. 3*E*, preincubation with hLIF-04 blocked the c-*fos* induction by human LIF, murine LIF, and by CT-1. By contrast, c-*fos* induction by PE was not affected by hLIF-04. Taken together, the results obtained with the anti-gp130 blocking antibody and the LIFRβ antagonist strongly suggest that CT-1, like LIF, requires both gp130 and LIFRβ to activate downstream signaling pathways leading to the induction of c-*fos* in cardiomyocytes.

CT-1 and LIF Induce Tyrosine Phosphorylation of gp130 and a 200-kDa Protein in Cardiomyocytes—To examine whether CT-1 would induce tyrosine phosphorylation of gp130, as it has been shown for the other members of the IL-6 cytokine family, cardiomyocytes were stimulated with soluble IL-6R, IL-6, a combination of IL-6 and sIL-6R, LIF, CT-1, and PE. Cell lysates were immunoprecipitated with a polyclonal anti-gp130 antiserum, analyzed by SDS-PAGE, and immunoblotted with an anti-phosphotyrosine antibody. As shown in Fig. 4*A*, the IL-6/sIL-6R complex, LIF, and CT-1 induced gp130 tyrosine phos-

[3] M. Saito and T. Taga, unpublished data.

phorylation. By contrast, no gp130 phosphorylation was detectable after stimulation with PE, and with IL-6 or sIL-6R alone. To compare the pattern of protein tyrosine phosphorylation induced by the various agonists, cell lysates were subjected to SDS-PAGE and immunoblotting with the anti-phosphotyrosine antibody (Fig. 4*B*). Stimulation with the IL-6/sIL-6R complex, LIF, and CT-1 resulted in the tyrosine phosphorylation of a protein, corresponding in size to gp130 (compare to Fig. 4*A*). An additional, higher molecular mass protein (approximately 200 kDa) was tyrosine-phosphorylated in response to LIF and CT-1 only, but not in response to the IL-6·sIL-6R complex.

CT-1 Induces a Morphologically Distinct Hypertrophic Response Characterized by the Assembly of Sarcomeric Units in Series—Neonatal rat ventricular cardiomyocytes respond to various hypertrophic stimuli by an increase in individual cell size, assembly of myofibrils, and perinuclear accumulation of ANF. To assess the effects of gp130/LIFRβ-dependent cytokines on these morphological features of a hypertrophic response, cardiomyocytes were treated with CT-1, LIF, or CNTF and dual-stained with an anti-TrpE/MLC-2v antiserum and a monoclonal anti-ANF antibody. Unstimulated cells and PE-treated cells served as negative and positive controls, respectively. The effects of CT-1, LIF, CNTF, and PE on cardiomyocyte area, length, and width and the percentage of cells displaying perinuclear accumulation of ANF are summarized in Table 1A. CT-1 and LIF induced a hypertrophic response, as evidenced by increases in cardiomyocyte area and the percentage of cells with perinuclear accumulation of immunoreactive ANF. As compared to PE stimulation, CT-1 and LIF had a more pronounced effect on cardiomyocyte length but did not significantly affect cardiomyocyte width. Treatment of cardiomyocytes with CNTF did not induce significant morphology changes as compared to control. Cardiomyocytes were dual-stained with a monoclonal anti-βMHC antibody and rhodamine phalloidine, to allow a simultaneous assessment of thick filament (βMHC) and thin filament (F-actin) assembly (56). Images were obtained by confocal laser microscopy. Representative high power fields are depicted in Fig. 5. Cardiomyocytes stimulated with CT-1 (*Panels E* and *F*) and LIF (*Panels G* and *H*) displayed a high degree of sarcomeric organization: myofibrils were oriented along the longitudinal cell axis, and extended into the tips of the cytoplasmic projections. As compared with PE stimulation (*Panels C* and *D*), sarcomeric units were assembled predominantly in series, rather than in parallel (most striking in cytoplasmic projections containing only a few myofibrils (see *Panels E–H*)). As shown in Table 1B, the average sarcomeric length did not differ significantly among the experimental groups.

CT-1 Induces ANF Gene Expression—The reactivation of an embryonic pattern of gene expression is a hallmark of cardiomyocyte hypertrophy. We therefore determined whether stimulation of cardiomyocytes with CT-1, LIF, or CNTF would induce embryonic gene expression (Fig. 6). As shown previously (11), stimulation of neonatal rat ventricular cardiomyocytes with PE resulted in a significant (5.1-fold) increase in prepro-ANF mRNA levels. Likewise, treatment with CT-1 or LIF stimulated prepro-ANF mRNA expression (5.1- and 5.0-fold, respectively). By contrast, CNTF did not significantly affect prepro-ANF mRNA levels. As previously reported (8), PE stimulation resulted in an increase (4.5-fold) in skeletal α-actin mRNA expression. CT-1, LIF, and CNTF, however, did not significantly affect skeletal α-actin steady state mRNA levels. Finally, we examined the effects of CT-1, LIF, CNTF, and PE on the expression of MLC-2v, a constitutively expressed contract-

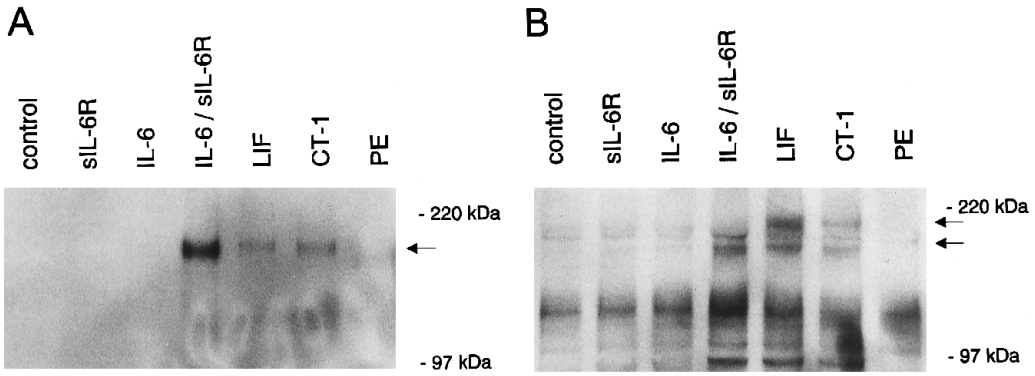

FIG. 4. **Protein tyrosine phosphorylation.** Neonatal rat ventricular cardiomyocytes were plated into 15-cm dishes and serum-starved for 18 h. Thereafter the cells were stimulated with sIL-6R, IL-6, IL-6 and sIL-6R combined, LIF, and CT-1 (10 nM each), or PE (100 μM) for 10 min at 37 °C. Cell lysates were immunoprecipitated with an anti-gp130 antibody, subjected to SDS-PAGE, and immunoblotting with an anti-phosphotyrosine antibody as outlined under "Experimental Procedures" (*Panel A*). In addition, cell lysates were directly subjected to SDS-PAGE and immunoblotting with an anti-phosphotyrosine antibody (*Panel B*).

TABLE I
Morphometric analysis

	Control	PE	CT-1	LIF	CNTF
Cell[a]					
Area (μm^2)	345 ± 17	635 ± 42*	543 ± 17*,#	508 ± 24*,#	305 ± 14§
Length (μm)	38 ± 1	56 ± 3*	74 ± 3*,§	79 ± 3*,§	38 ± 1§
Width (μm)	22 ± 1	29 ± 1*	23 ± 1§	23 ± 1§	21 ± 1§
ANF positive (%)	6	51	32	26	6
Sarcomere[b]					
Length (μm)	1.72 ± 0.07	1.73 ± 0.07	1.72 ± 0.06	1.70 ± 0.05	1.71 ± 0.08

[a] Neonatal rat ventricular cardiomyocytes were plated into chamber slides and incubated with no additions (control), PE (100 μM), CT-1, LIF, or CNTF (1 nM each). After 48 h, the cells were immunostained against MLC-2v and ANF. Cell area, length, and width were measured in 50–60 MLC-2v-positive cells from six randomly chosen high power fields per condition. Values are means ± S.E.; * $p < 0.0001$ *versus* control; # $p < 0.01$ *versus* PE; § $p < 0.0001$ *versus* PE. In addition, 250 cells from each group were scored for MLC-2v and ANF expression, and the percentage of MLC-2v positive cells that displayed perinuclear staining for immunoreactive ANF was calculated.

[b] Twenty sarcomere segments were measured in each of 8–10 randomly chosen cardiomyocytes stained against βMHC, and viewed by confocal laser microscopy. Values are means ± S.E.; p = not significant.

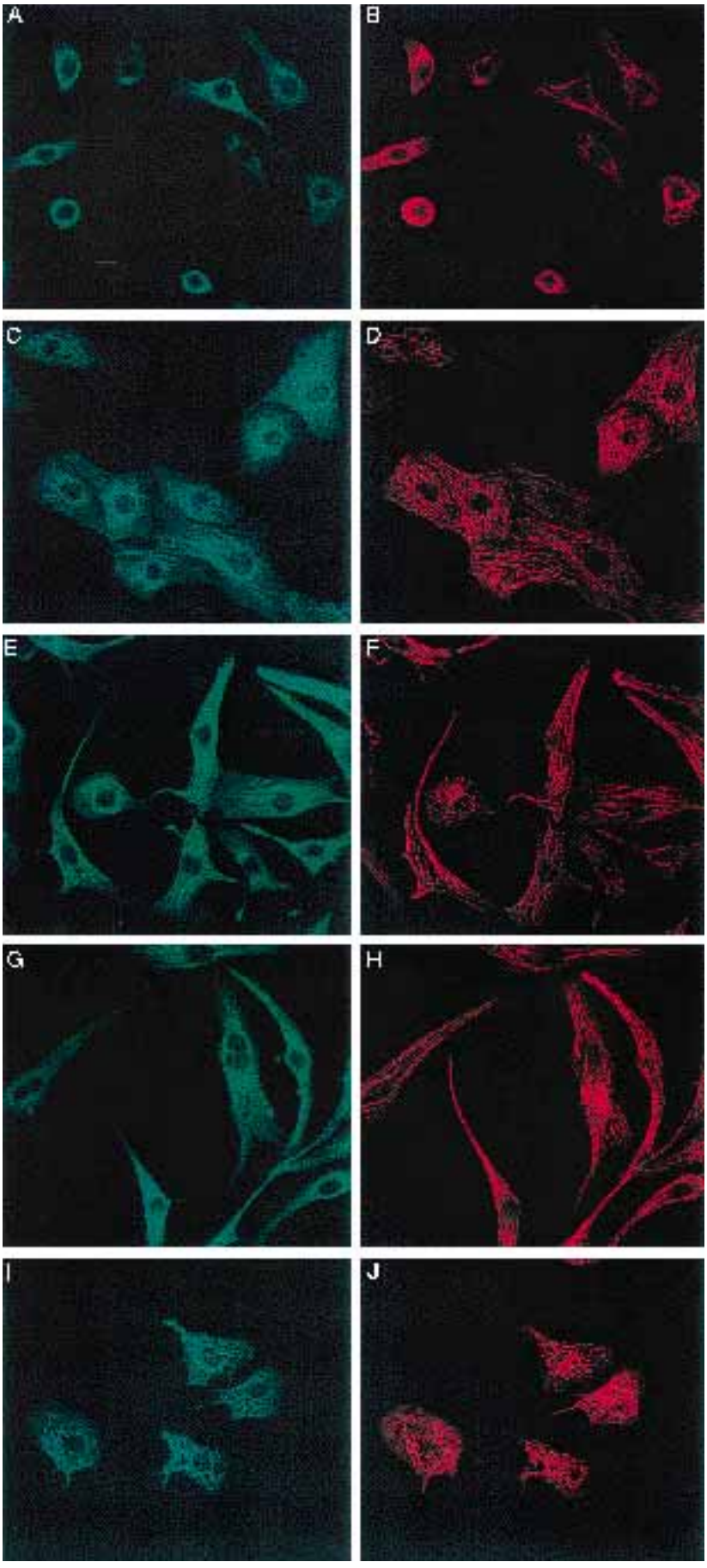

FIG. 5. **Sarcomeric organization.** Neonatal rat ventricular cardiomyocytes were plated into chamber slides and incubated for 48 h with no additions (*Panels A* and *B*), 100 μM PE (*Panels C* and *D*), 1 nM CT-1 (*Panels E* and *F*), 1 nM LIF (*Panels G* and *H*), or 1 nM CNTF (*Panels I* and *J*). Cells were dual-labeled with an anti-βMHC antibody (*Panels A*, *C*, *E*, *G*, and *I*) and rhodamine phalloidine (*Panels B*, *D*, *F*, *H*, and *J*), and viewed by confocal laser microscopy. The *bar* (*Panel A*) represents 10 μm.

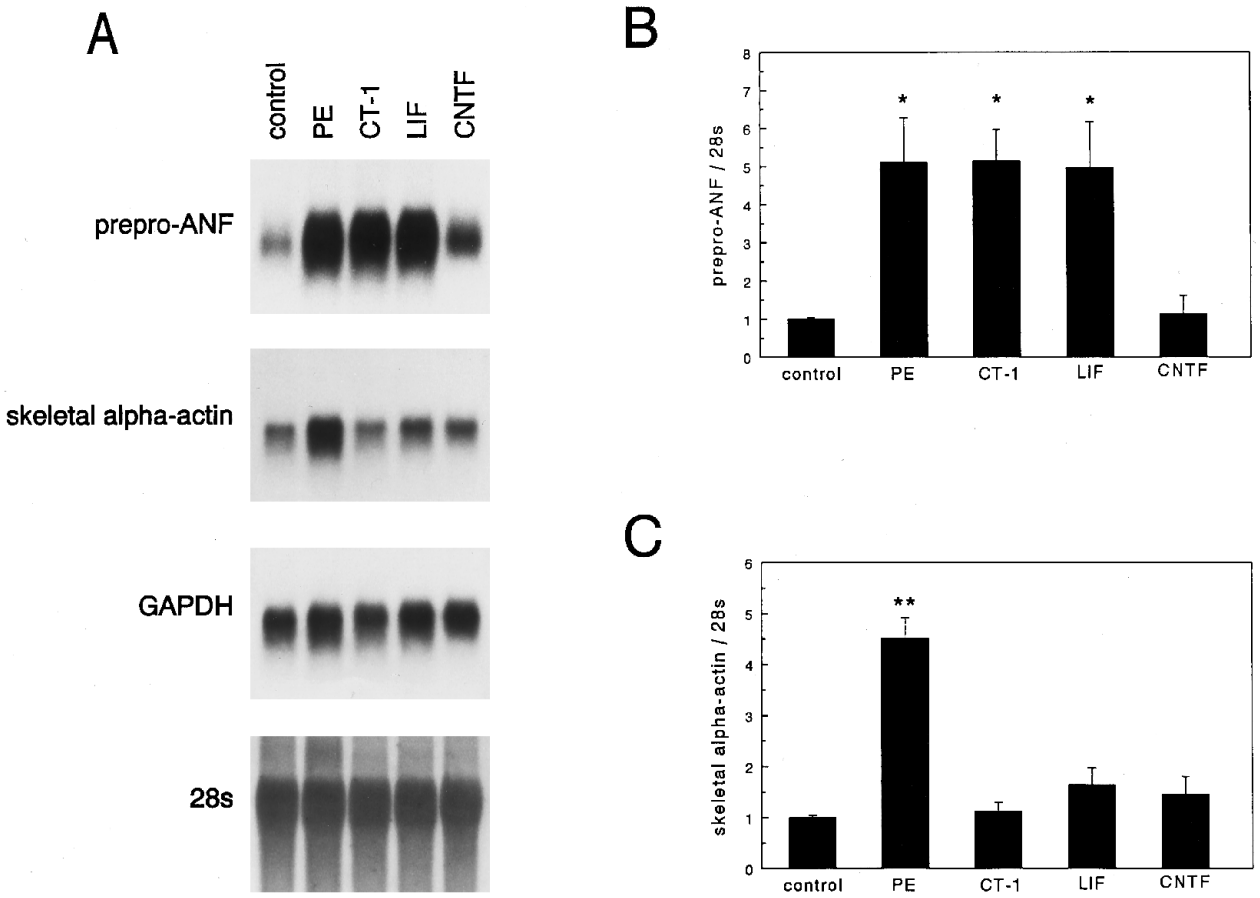

FIG. 6. **Expression of prepro-ANF and skeletal α-actin mRNAs.** Neonatal rat ventricular cardiomyocytes were plated into 15-cm dishes and incubated for 48 h with no additions (*control*), PE (100 μM), CT-1, LIF, or CNTF (1 nM each). Total RNA was isolated and subjected to Northern blot analysis (10 μg/lane) using prepro-ANF and skeletal α-actin cDNA probes. Equal loading and transfer conditions were confirmed by GAPDH and 28s hybridization. Representative blots are presented in *Panel A*. The results from three independent experiments, expressed as -fold induction over control, are depicted in *Panels B* and *C*. Values are means ± S.E.; $*p < 0.05$, $**p < 0.01$ *versus* control.

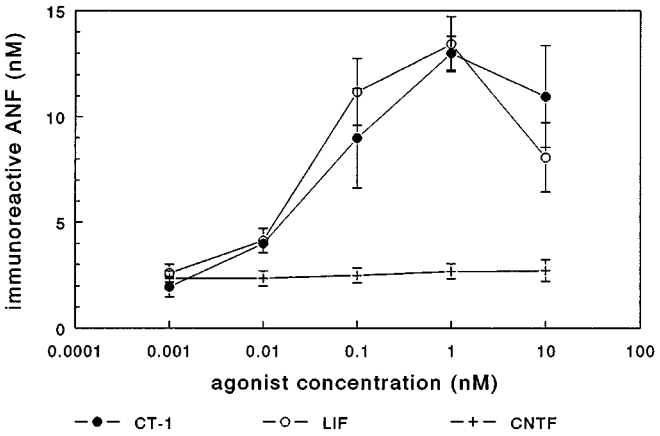

FIG. 7. **Release of immunoreactive ANF from myocardial cells.** Neonatal rat ventricular cardiomyocytes were cultured in 24- well plates, and stimulated for 48 h with various concentrations of CT-1, LIF, and CNTF. ANF concentrations in the culture supernatants were determined by radioimmunoassay. Values are means ± S.E. from triplicate wells. Supernatants from unstimulated control cells and PE (100 μM) stimulated cells contained 2.5 ± 0.4 nM and 20.8 ± 1.5 nM ANF, respectively. Two additional experiments yielded comparable results.

ile protein gene. PE stimulation resulted in a marginal 1.5-fold induction of MLC-2v mRNA levels. By contrast, CT-1, LIF, and CNTF did not induce MLC-2v mRNA expression (data not shown). We next determined whether the increase in prepro-ANF mRNA expression in response to CT-1 and LIF is accompanied by an increase in secretion of immunoreactive ANF. As noted in the initial study reporting the cloning of CT-1 (19), CT-1 induced ANF release from cardiomyocytes in a dose-dependent manner (Fig. 7). Likewise, LIF increased the secretion of ANF; maximum ANF release was observed with CT-1 and LIF concentrations of 0.1–10 nM. Consistent with the ANF Northern blot results, stimulation with CNTF did not induce ANF release at any of the concentrations tested (Fig. 7).

CT-1 Activates the Transcription of the ANF Gene—To determine whether the induction of ANF by CT-1 results from an increased ANF gene transcription, we performed nuclear run-on transcription assays. We compared the ANF gene transcription rate during stimulation with CT-1 and PE. A typical experiment is presented in Table II and Fig. 8. Cardiomyocyte nuclei were isolated at various time points during stimulation with CT-1 or PE. Unstimulated cells served as a control. CT-1 and PE increased the overall RNA transcription rate, as measured by the total amount of ^{32}P incorporation into purified run-on RNA (Table II). The overall RNA transcription rate was higher at the early time points (0, 6, and 12 h), *i.e.* shortly after serum withdrawal (Table II). An equal number of cpm from each run-on reaction was hybridized to denatured prepro-ANF and GAPDH cDNAs immobilized onto nylon filters. The ANF autoradiograms are shown in Fig. 8*A*. The CT-1 and PE induced ANF transcription rates were calculated as -fold induction over the corresponding control values from each time point (Fig. 8*B*). ANF transcription reached a maximum 2.0-fold (CT-1) and 2.1-fold (PE) increase *versus* control at 24 h and returned to control levels at 48 h. By contrast, GAPDH gene transcription was not affected by CT-1 or PE (not shown). The

TABLE II

Total RNA transcription in control cells and CT-1- or phenylephrine-stimulated cells

Neonatal rat ventricular cardiomyocytes were plated into 15-cm dishes (10×10^6 cells/dish), allowed to attach overnight, and switched to maintenance medium. Thereafter, nuclei from one dish were harvested (0 h, control). The remaining cells were further incubated with no additions (controls), 1 nM CT-1, or 100 μM PE. Cardiomyocyte nuclei were isolated at the indicated time points, and nuclear run-on transcription assays were performed as described under "Experimental Procedures." The total amount of ^{32}P incorporation into purified run-on RNA was determined by liquid scintillation counting as an index of overall transcriptional activity. Data are presented as cpm $\times 10^6$.

	Incubation					
	0 h	6 h	12 h	18 h	24 h	48 h
Control	5.2	2.9	2.4	1.7	1.3	1.4
CT-1		3.3	3.8	2.3	2.4	1.8
PE		5.3	3.7	1.9	1.8	1.4

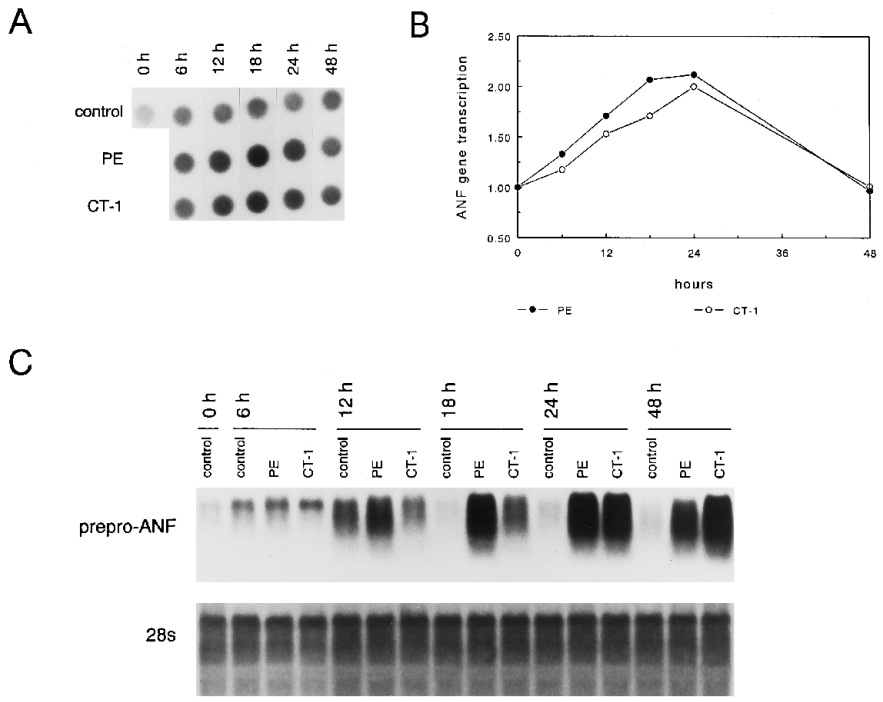

FIG. 8. **CT-1- and phenylephrine-induced ANF gene transcription.** Same experiment as described in Table II. 1.2×10^6 cpm from each run-on reaction were hybridized to linearized and denatured pBluescript harboring the prepro-ANF cDNA, immobolized onto nylon filters. The filters were washed under stringent conditions, and exposed to x-ray film for 5 days (*Panel A*). The signal intensities were analyzed by densitometry to quantitate the amount of ANF gene transcription; data are presented as -fold induction over control (*Panel B*). Total RNA was isolated from the cytosolic fractions of the same cells, that were used for the run-on assays. RNA was subjected to Northern blot analysis (7.5 μg/lane), using prepro-ANF and 28s cDNA probes (*Panel C*). Data from one experiment are presented. One additional experiment yielded comparable results.

CT-1- and PE-induced increase in ANF gene transcription was accompanied by a time-dependent accumulation of prepro-ANF mRNA in the cytosol, reaching maximum levels between 24 and 48 h (Fig. 8*C*). By contrast, CT-1 and PE did not affect GAPDH mRNA expression (not shown).

CT-1 Responsive Cis-regulatory Sequences Are Located Outside a 3003-bp ANF Promoter Fragment—The transcriptional up-regulation of the ANF gene in response to a number of G-protein coupled receptor agonists, including PE, is mediated by *cis*-regulatory elements, which are located within the proximal 3 kb of ANF 5′-flanking region (11, 12, 57). We performed transient transfection analyses to determine whether gp130/LIFRβ-dependent cytokines and PE utilize common *cis*-acting elements within the ANF promoter region. Cardiomyocytes were transfected with an ANF-luciferase reporter construct containing 3003 bp of the rat ANF 5′-flanking region. Cardiomyocytes transfected with a RSV-luciferase construct or a promoterless luciferase construct were used as positive and negative controls, respectively. To control for transfection efficiency, cells were cotransfected with a β-galactosidase expression vector. The cells were then stimulated with PE, CT-1, LIF, or CNTF; unstimulated cells served as controls. At various time points, cardiomyocytes were harvested for luciferase and β-galactosidase assays. As previously reported (11), the 3003-bp ANF promoter fragment conferred PE-inducible expression to the luciferase reporter gene (maximum 23.7-fold induction at 48 h) (Fig. 9). By contrast, the 3003-bp ANF promoter fragment did not mediate inducible expression by CT-1, LIF, or CNTF (Fig. 9). Luciferase activities in cells transfected with the RSV-luciferase construct were on average 80-fold higher as compared to unstimulated cells transfected with the ANF-luciferase construct and were not induced by any of the treatments (not shown). Cells transfected with the promoterless reporter construct displayed luciferase activities that were not different from background values and were not affected by any of the treatments (not shown). Considering that CT-1 as well as PE increase the ANF gene transcription rate (as demonstrated by nuclear run-on assays), the transfection analyses suggest that, in contrast to PE, the CT-1 responsive *cis*-regulatory elements are located outside of 3 kb of ANF 5′-flanking region. Thus, divergent pathways appear to mediate the induction of the ANF gene in response to CT-1 as compared to α-adrenergic stimulation.

DISCUSSION

CT-1 Signaling through the gp130/LIFRβ Heterodimer—Cardiotrophin-1 was recently isolated by expression cloning based on its ability to induce an increase in cell size in cardiomyocyte culture (19). The deduced amino acid sequence suggested that CT-1 is a novel member of the IL-6, IL-11, LIF, CNTF, and OSM family of structurally related cytokines, that trigger downstream signaling pathways in multiple cell types through the homodimerization of gp130 or the heterodimerization of gp130 and LIFRβ (22, 24, 26, 27). To determine whether CT-1 shares the receptor components gp130 and/or LIFRβ with the other members of the IL-6 cytokine family, we employed a

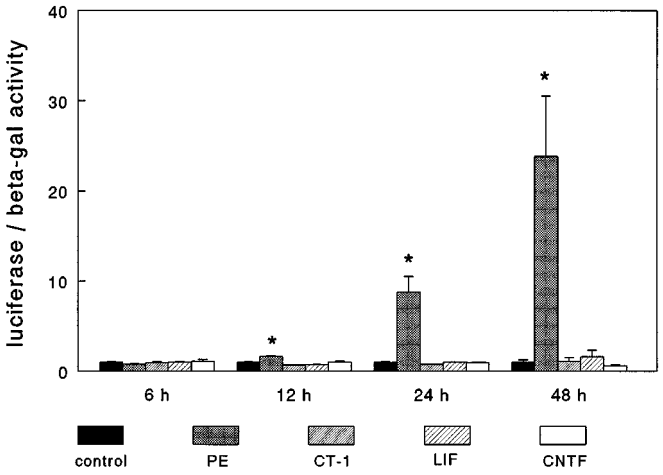

FIG. 9. **Transient transfection analysis of a 3003- bp ANF promoter-luciferase reporter construct.** Neonatal rat ventricular cardiomyocytes were cotransfected with an ANF-luciferase reporter construct (pANF(−3003)Luc5′) and a β-galactosidase control vector (pON249), and incubated with no additions (*control*), PE (100 μM), CT-1, LIF, or CNTF (1 nM each). At the indicated time points, cells were harvested for luciferase and β-galactosidase assays. Luciferase activities were normalized to β-galactosidase activities. Results are presented as -fold induction over control cells harvested at corresponding time points. Values are means ± S.E. of four experiments at each time point; $*p < 0.01$ *versus* control.

monoclonal anti-gp130 antibody and a mutated human LIF protein, acting as a LIFRβ antagonist. The c-*fos* induction by CT-1 and LIF in cardiomyocytes was antagonized by the monoclonal anti-gp130 antibody as well as the LIFRβ antagonist, strongly suggesting that CT-1, like LIF, utilizes the receptor components gp130 and LIFRβ. As demonstrated by gp130 immunoprecipitation and subsequent anti-phosphotyrosine immunoblotting, stimulation of cardiomyocytes with CT-1, LIF, and a combination of IL-6 and sIL-6R resulted in the rapid tyrosine phosphorylation of gp130. These data indicate that tyrosine phosphorylation of gp130 is an early step in CT-1 signaling, as it has previously been shown for the other members of the IL-6 cytokine family (21–23). As determined by immunoblotting with an anti-phosphotyrosine antibody, LIF induced the tyrosine phosphorylation of an additional ~200 kDa protein, which was not phosphorylated upon stimulation with the IL-6/sIL-6R complex. Based on previous results, this protein most likely corresponds to LIFRβ (22, 26, 58). Stimulation of cardiac cells with CT-1 resulted in the tyrosine phosphorylation of a protein, indistinguishable in size from LIFRβ, as well. Considering the ability of the LIFRβ antagonist to block the action of CT-1 in cardiomyocytes, the immunoblotting results strongly suggest that CT-1, like LIF, induces the tyrosine phosphorylation of LIFRβ. In support of this conclusion, CT-1 has recently been shown to bind to purified LIFRβ in solution with about the same affinity as LIF, and to interact with a cell surface protein in M1 cells with a mobility expected for LIFRβ (54). In summary, the present study indicates that CT-1 signals through and induces tyrosine phosphorylation of the gp130/LIFRβ heterodimer in cardiomyocytes.

CT-1 Induces a Hypertrophic Phenotype in Cultured Myocardial Cells Characterized by Sarcomere Assembly in Series and a Selective Up-regulation of ANF Gene Expression—The present study provides clear evidence that the CT-1 induced hypertrophic phenotype is distinct from the hypertrophic phenotype observed following G-protein-dependent stimulation. On a single cell level, G-protein-dependent pathways induce a form of hypertrophy with a relatively uniform increase in myocyte size and the addition of new myofibrils in parallel (12, 15, 16). By contrast, as noted in the present study, the gp130/LIFRβ-dependent cytokines CT-1 and LIF induce an increase in myocyte size characterized by a marked increase in cell length, but little or no change in cell width. To characterize the effects of gp130/LIFRβ-dependent stimulation on the myofibrillar cytoarchitecture, cardiomyocytes were dual-stained against thick (βMHC) and thin (F-actin) myofilaments, and viewed by confocal laser microscopy (56). Cardiomyocytes stimulated with CT-1 and LIF displayed a high degree of myofibrillar organization; myofibrils were organized in a strictly sarcomeric pattern, were oriented along the longitudinal cell axis, and extended to the cell periphery. Importantly, the increase in cell size and length was associated with no change in the average sarcomere length, strongly suggesting that the cell elongation in response to gp130/LIFRβ-dependent stimulation results from an addition of new sarcomeric units in series. The morphologic changes induced by gp130/LIFRβ-dependent stimulation *in vitro* are reminiscent of the changes observed in cardiac myocytes isolated from hearts subjected to chronic volume overload (3, 4). By contrast, the pattern of cardiomyocyte hypertrophy induced by α-adrenergic stimulation more closely resembles a pressure overload-like phenotype (1, 2).

On a molecular level, gp130/LIFRβ-dependent stimulation and α-adrenergic stimulation resulted in distinct patterns of embryonic gene, MLC-2v, and immediate early gene expression. Stimulation of cardiomyocytes with CT-1 and LIF induced prepro-ANF mRNA expression, and perinuclear accumulation and secretion of immunoreactive ANF. However, in contrast to α-adrenergic stimulation, CT-1 and LIF did not induce skeletal α-actin expression. Growth factors, signaling through G-protein coupled receptors induce ANF and skeletal α-actin in a coordinate fashion (8, 11–14). A recent study compared the expression pattern of distinct members of the embryonic gene program in pressure overload *versus* volume overload hypertrophy *in vivo* in the rat myocardium (5). As shown previously (52), pressure overload resulted in the coordinate induction of ANF and skeletal α-actin. However, volume overload hypertrophy was associated with a selective increase in ANF expression, and no induction of skeletal α-actin, suggesting that the regulation of distinct embryonic genes *in vivo* is related to the hypertrophic stimulus (5). The pattern of embryonic gene expression induced by CT-1 and LIF in cardiomyocyte culture therefore resembles the pattern observed in volume overload hypertrophy *in vivo*.

Nuclear run-on transcription assays revealed that the induction of prepro-ANF mRNA by CT-1 and α-adrenergic stimulation is mediated, at least in part, by an increased transcription of the ANF gene. The fact that the ANF mRNA levels increased 5-fold, whereas the ANF gene transcription rate increased only 2-fold, suggests that post-transcriptional mechanisms(s) participate in the up-regulation of ANF gene expression in response to CT-1 and PE (59). In agreement with previous results (11), a 3003-bp ANF promoter fragment conferred PE-inducible expression to a luciferase reporter gene. Likewise, the *cis*-regulatory elements mediating ANF inducibility in response to endothelin 1 and α-thrombin reside within the proximal 3 kb of the ANF 5′-flanking region, suggesting that G-protein-coupled receptor agonists may utilize common signaling pathways for the induction of ANF (12, 57). By contrast, none of the gp130/LIFRβ-dependent cytokines (CT-1, LIF, and CNTF) activated the 3003-bp ANF promoter fragment. Considering the increased ANF gene transcription rate in response to CT-1 and PE, we conclude that in contrast to α-adrenergic stimulation, the CT-1 responsive *cis*-regulatory elements are located outside of the proximal 3 kb of the ANF 5′-flanking region. In recent studies, transgenic mice harboring 3003 bp of ANF 5′-flanking region upstream of a luciferase reporter gene were subjected to

transverse aortic banding. Despite a marked increase in left ventricular prepro-ANF mRNA expression, no significant increase in reporter activity was observed (60). These findings demonstrate that the induction of ANF during cardiac hypertrophy *in vivo* occurs through a distinct mechanism as compared to G-protein-mediated cardiomyocyte hypertrophy *in vitro*. Unraveling the mechanisms of ANF induction in response to gp130/LIFRβ-dependent stimulation may therefore provide insight into the mechanisms governing the induction of ANF during *in vivo* cardiac hypertrophy.

CT-1 and LIF did not induce MLC-2v mRNA expression, whereas phenylephrine stimulation resulted in a marginal induction of MLC-2v. The induction of MLC-2v on the mRNA level may be a feature unique to G-protein-coupled receptor stimulation of cardiomyocytes *in vitro* (10, 12): MLC-2v mRNA expression is not up-regulated in the hypertrophic right ventricles of pulmonary artery-banded mice (61) and in the hypertrophic ventricles of transgenic mice overexpressing a constitutively active α-adrenergic receptor in the myocardium (62).

A distinct response to gp130/LIFRβ-dependent *versus* α-adrenergic stimulation was also observed at the level of immediate early gene induction. As compared to α-adrenergic stimulation, CT-1 and LIF induced >10-fold higher levels of c-*myc* and *tis11* expression. Immediate early genes encode known or putative transcription factors, and potential binding sites have been identified in the promoter regions of a number of cardiac genes (for review, see Ref. 63). The distinct combinatorial expression of immediate early genes may therefore relate to the differences in cell morphology and gene expression pattern in response to gp130/LIFRβ-dependent *versus* α-adrenergic stimulation.

Taken together, these studies indicate that gp130/LIFRβ-dependent pathways can activate a hypertrophic phenotype in cardiac muscle cells which is distinct both at a morphological and a molecular level from the phenotype seen following G-protein-dependent stimulation, and that is more consistent with a volume overload, as opposed to pressure overload, hypertrophic phenotype. Future studies in transgenic mice will be required to rigorously test whether gp130/LIFRβ-dependent signaling pathways are implicated in volume overload and/or pressure overload ventricular hypertrophy *in vivo*, in a manner analogous to recent studies exploring the *in vivo* role of *ras*-dependent pathways (18). In this regard, double transgenic mice overexpressing IL-6 and IL-6R have recently been generated (64). These mice display a constitutive tyrosine phosphorylation (*i.e.* activation) of gp130 in the myocardium and left ventricular hypertrophy with increases in cardiac weights and cardiomyocyte volumes. These results suggest that the induction of cardiomyocyte hypertrophy through gp130-dependent signaling pathways is not confined to the *in vitro* hypertrophy assay, but may also be observed in the *in vivo* context.

The question arises as to the relative role of individual members of the IL-6 cytokine family in the activation of a hypertrophic response *in vivo*. The expression of IL-6R in the heart of wild type mice is extremely low, making IL-6 an unlikely mediator of cardiac hypertrophy *in vivo*.[4] Accordingly, a combination of IL-6 with sIL-6R was required to induce tyrosine phosphorylation of gp130 in cardiomyocytes in the present study. Likewise, the myocardium does not express substantial levels of CNTFRα (30), and cardiomyocytes did not respond to CNTF stimulation in the present study. It should be noted, however, that CNTF exerted marginal effects on immediate early gene expression in cardiomyocytes. This might relate to a weak interaction of CNTF with the gp130/LIFRβ heterodimer in the absence of CNTFRα (65, 66). Alternatively, low level expression of CNTFRα in cardiomyocytes may account for a weak responsiveness to CNTF. The CT-1 mRNA is expressed in the heart from adult mice (19). RNase protection analysis of cardiac muscle cells and cardiac-derived fibroblasts from neonatal rats reveals a >10-fold higher level of CT-1 mRNA expression in cardiac muscle cells *versus* cardiac fibroblasts, and CT-1 is expressed primarily in cardiac muscle cells during murine cardiogenesis (67). By contrast, the expression of LIF mRNA in the adult murine heart is extremely low as documented by RNase protection analysis (68, 69). These data would suggest that CT-1 is a candidate cytokine activating gp130/LIFRβ-dependent signaling pathways within the myocardium, potentially through an autocrine pathway. The generation of mice containing a null-mutation of the CT-1 gene should provide a more definitive understanding of the *in vivo* role of CT-1 in development and in cardiac hypertrophy in the adult animal.

Acknowledgments—We gratefully acknowledge Dr. Peter Gruber for helping with the confocal laser microscopy and Dr. Nicholas F. Paoni for supplying us with CT-1.

REFERENCES

1. Morkin, E. (1970) *Science* **167,** 1499–1501
2. Anversa, P., Ricci, R., and Olivetti, G. (1986) *J. Am. Coll. Cardiol.* **7,** 1140–1149
3. Anversa, P., Levicky, V., Beghi, C., McDonald, S. L., and Kikkawa, Y. (1983) *Circ. Res.* **52,** 57–64
4. Gerdes, A. M., Campbell, S. E., and Hilbelink, D. R. (1988) *Lab. Invest.* **59,** 857–861
5. Calderone, A., Takahashi, N., Izzo, N. J., Thaik, C. M., and Colucci, W. S. (1995) *Circulation* **92,** 2385–2390
6. Simpson P., McGrath, A., and Savion, S. (1982) *Circ. Res.* **51,** 787–801
7. Simpson, P. and McGrath, A. (1983) *J. Clin. Invest.* **72,** 732–738
8. Bishopric, N. H., Simpson, P. C., and Ordahl, C. P. (1987) *J. Clin. Invest.* **80,** 1194–1199
9. Long, C. S., Ordahl, C. P., and Simpson, P. C. (1989) *J. Clin. Invest.* **83,** 1078–1082
10. Lee, H. R., Henderson, S. A., Reynolds, R., Dunnmon, P., Yuan, D., and Chien, K. R. (1988) *J. Biol. Chem.* **263,** 7352–7358
11. Knowlton, K. U., Baracchini, E., Ross, R. S., Harris, A. N., Henderson, S. A., Evans, S. M., Glembotski, C. C., and Chien, K. R. (1991) *J. Biol. Chem.* **266,** 7759–7768
12. Shubeita, H. E., McDonough, P. M., Harris, A. N., Knowlton, K. U., Glembotski, C. C., Brown, J. H., and Chien, K. R. (1990) *J. Biol. Chem.* **265,** 20555–20562
13. Ito, H., Hirata, Y., Hiroe, M., Tsujino, M., Adachi, S., Takamoto, T., Nitta, M., Taniguchi, K., and Marumo, F. (1991) *Circ. Res.* **69,** 209–215
14. Sadoshima, J., and Izumo, S. (1993) *Circ. Res.* **73,** 413–423
15. Iwaki, K., Sukhatme, V. P., Shubeita, H. E., and Chien, K. R. (1990) *J. Biol. Chem.* **265,** 13809–13817
16. Knowlton, K. U., Michel, M. C., Itani, M, Shubeita, H. E., Ishihara, K., Brown, J. H., and Chien, K. R. (1993) *J. Biol. Chem.* **268,** 15374–15380
17. Thorburn, A., Thorburn, J., Chen, S., Powers, S., Shubeita, H. E., Feramisco, J. R., and Chien, K. R. (1993) *J. Biol. Chem.* **268,** 2244–2249
18. Hunter, J., Tanaka, N., Rockman, H. A., Ross, J., Jr., and Chien, K. R. (1995) *J. Biol. Chem.* **270,** 23173–23178
19. Pennica, D., King, K. L., Shaw, K. J., Luis, E., Rullamas, J., Luoh, S., Darbonne, W. C., Knutzon, D. S., Yen, R., Chien, K. R., Baker, J. B., and Wood, W. I. (1995) *Proc. Natl. Acad. Sci. U. S. A.* **92,** 1142–1146
20. Hibi, M., Murakami, M., Saito, M., Hirano, T., Taga, T., and Kishimoto, T. (1990) *Cell* **63,** 1149–1157
21. Taga, T., Narazaki, M., Yasukawa, K., Saito, T., Miki, D., Hamaguchi, M., Davis, S., Shoyab, M., Yancopoulos, G. D., and Kishimoto, T. (1992) *Proc. Natl. Acad. Sci. U. S. A.* **89,** 10998–11001
22. Ip, N. Y., Nye, S. H., Boulton, T. G., Davis, S., Taga, T., Li, Y., Birren, S. J., Yasukawa, K., Kishimoto, T., Anderson, D. J., Stahl, N., and Yancopoulos, G. D. (1992) *Cell* **69,** 1121–1132
23. Yin, T., Taga, T., Tsang, M. L., Yasukawa, K., Kishimoto, T., and Yang, Y. (1993) *J. Immunol.* **151,** 2555–2561
24. Murakami, M., Hibi, M., Nakagawa, N., Nakagawa, T., Yasukawa, K., Yamanishi, K., Taga, T., and Kishimoto, T. (1993) *Science* **260,** 1808–1810
25. Gearing, D. P., Thut, C. J., VandenBos, T., Gimpel, S. D., Delaney, P. B., King, J., Price, V., Cosman, D., and Beckmann, M. P. (1991) *EMBO J.* **10,** 2839–2848
26. Davis, S., Aldrich, T. H., Stahl, N., Pan, L., Taga, T., Kishimoto, T., Ip, N. Y., and Yancopoulos, G. D. (1993) *Science* **260,** 1805–1808
27. Gearing, D. P., Comeau, M. R., Friend, D. J., Gimpel, S. D., Thut, C. J., McGourty, J., Brasher, K. K., King, J. A., Gillis, S., Mosley, B., Ziegler, S. F., and Cosman, D. (1992) *Science* **255,** 1434–1437
28. Yamasaki, K., Taga, T., Hirata, Y., Yawata, H., Kawanishi, Y., Seed, B., Taniguchi, T., Hirano, T., and Kishimoto, T. (1988) *Science* **241,** 825–828
29. Taga, T., Hibi, M., Hirata, Y., Yamasaki, K., Yasukawa, K., Matsuda, T., Hirano, T., and Kishimoto, T. (1989) *Cell* **58,** 573–581
30. Davis, S., Aldrich, T. H., Valenzuela, D. M., Wong, V., Furth, M. E., Squinto, S. P., and Yancopoulos, G. D. (1991) *Science* **253,** 59–63

[4] T. Kishimoto, personal communication.

31. Ip, N. Y., McClain, J., Barrezueta, N. X., Aldrich, T. H., Pan, L., Li, Y., Wiegand, S. J., Friedman, B., Davis, S., and Yancopoulos, G. D. (1993) *Neuron* **10,** 89–102
32. Robinson, R. C., Grey, L. M., Staunton, D., Vankelecom, H., Vernallis, A. B., Moreau, J. F., Stuart, D. I., Heath, J. K., and Jones, E. Y. (1994) *Cell* **77,** 1101–1116
33. Henderson, S. A., Spencer, M., Sen, A., Kumar, C., Siddiqui, M. A. Q., and Chien, K. R. (1989) *J. Biol. Chem.* **264,** 18142–18148
34. Hirata, Y., Taga, T., Hibi, M., Nakano, N, and Kishimoto, T. (1989) *J. Immunol.* **143,** 2900–2906
35. Glembotski, C. C., Oronzi, M. E., Li, X., Shields, P. P., Johnston, J. F., Kallen, R. G., and Gibson, T. R. (1987) *Endocinology* **121,** 843–852
36. Shields, P. P., and Glembotski, C. C. (1988) *J. Biol. Chem.* **263,** 8091–8098
37. Bouvagnet, P., Leger, J., Pons, F., Dechesne, C. A., and Leger, J. J. (1984) *Circ. Res.* **55,** 794–804
38. Chomczynski, P., and Sacchi, N. (1987) *Anal. Biochem.* **162,** 156–159
39. Van Beveren, C., van Straaten, F., Curran, T., Müller, R., and Verma, I. M. (1983) *Cell* **32,** 1241–1255
40. Christy, B. A., Lau, L. F., and Nathans, D. (1988) *Proc. Natl. Acad. Sci. U. S. A.* **85,** 7857–7861
41. Ryder, K., and Nathans, D. (1988) *Proc. Natl. Acad. Sci. U. S. A.* **85,** 8464–8467
42. Ryder, K., Lau, L. F., and Nathans, D. (1988) *Proc. Natl. Acad. Sci. U. S. A.* **85,** 1487–1491
43. Lim, R. W., Varnum, B. C., and Herschman, H. R. (1987) *Oncogene* **1,** 263–270
44. Seidman, C. E., Duby, A. D., Choi, E., Graham, R. M., Haber, E., Homcy, C., Smith, J. A., and Seidman, J. G. (1984) *Science* **225,** 324–326
45. Shani, M., Nudel, U., Zevin-Sonkin, D., Zakut, R., Givol, D., Katcoff, D., Carmon, Y., Reiter, J., Frischauf, A. M., and Yaffe, D. (1981) *Nucleic Acids Res.* **9,** 579–589
46. Henderson, S. A., Xu, Y., and Chien, K. R. (1988) *Nucleic Acids Res.* **16,** 4722
47. Adams, M. D., Dubnick, M., Kerlavage, A. R., Moreno, R., Kelley, J. M., Utterback, T. R., Nagle, J. W., Fields, C., and Venter, J. C. (1992) *Nature* **355,** 632–634
48. Marzluff, W. F., and Huang, R. C. C. (1985) in *Transcription and Translation: A Practical Approach* (Harnes, B. D., and Higgins, S. J., eds) pp. 89–129, IRL Press, Oxford
49. deWet, J. R., Wood, K. V., DeLuca, M., Helinski, D. R., and Subramani, S. (1987) *Mol. Cell. Biol.* **7,** 725–737
50. Cherrington, J. M., and Mocarski, E. S. (1989) *J. Virol.* **63,** 1435–1440
51. Chen, C., and Okayama, H. (1987) *Mol. Cell. Biol.* **7,** 2745–2752
52. Izumo, S., Nadal-Ginard, B., and Mahdavi, V. (1988) *Proc. Natl. Acad. Sci. U. S. A.* **85,** 339–343
53. Rockman, H. A., Ross, R. S., Harris, A. N., Knowlton, K. U., Steinhelper, M. E., Field, L. J., Ross, J., and Chien, K. R. (1991) *Proc. Natl. Acad. Sci. U. S. A.* **88,** 8277–8281
54. Pennica, D., Shaw, K. J., Swanson, T. A., Moore, M. W., Shelton, D. L., Zioncheck, K. A., Rosenthal, A., Taga, T., Paoni, N. F., and Wood, W. I. (1995) *J. Biol. Chem.* **270,** 10915–10922
55. Seidman, C. E., Schmidt, E. V., and Seidman, J. G. (1991) *Can. J. Physiol. Pharmacol.* **69,** 1486–1492
56. Messerli, J. M., Eppenberger-Eberhardt, M. E., Rutishauser, B. M., Schwarb, P., von Arx, P., Koch-Schneidemann, S., Eppenberger, H. M., and Perriard, J. C. (1993) *Histochemistry* **100,** 193–202
57. Glembotski, C. C., Irons, C. E., Krown, K. A., Murray, S. F., Sprenkle, A. B., and Sei, C. A. (1993) *J. Biol. Chem.* **268,** 20646–20652
58. Boulton, T. G., Stahl, N., and Yancopoulos, G. D. (1994) *J. Biol. Chem.* **269,** 11648–11655
59. Hargrove, J. L. (1993) *FASEB J.* **7,** 1163–1170
60. Knowlton, K. U., Rockman, H. A., Itani, M., Vovan, A., Seidman, C. E., and Chien, K. R. (1995) *J. Clin. Invest.* **96,** 1311–1318
61. Rockman, H. A., Ono, S., Ross, R. S., Jones, L. R., Karimi, M., Bhargava, V., Ross, J., and Chien, K. R. (1994) *Proc. Natl. Acad. Sci. U. S. A.* **91,** 2694–2698
62. Milano, C. A., Dolber, P. C., Rockman, H. A., Bond, R. A., Venable, M. E., Allen, L. F., and Lefkowitz, R. J. (1994) *Proc. Natl. Acad. Sci. U. S. A.* **91,** 10109–10113
63. Chien, K. R., Zhu, H., Knowlton, K. U., Miller-Hance, W., van Bilsen, M., O'Brien, T. X., and Evans, S. (1993) *Annu. Rev. Physiol.* **55,** 77–95
64. Hirota, H., Yoshida, K., Kishimoto, T., and Taga, T. (1995) *Proc. Natl. Acad. Sci. U. S. A.* **92,** 4862–4866
65. Davis, S., Aldrich, T. H., Ip, N. Y., Stahl, N., Scherer, S., Farruggella, T., DiStefano, P. S., Curtis, R., Panayotatos, N., Gascan, H., Chevalier, S., and Yancopoulos, G. D. (1993) *Science* **259,** 1736–1739
66. Gearing, D. P., Ziegler, S. F., Comeau, M. R., Friend, D. Thoma, B., Cosman, D., Park, L., and Mosley, B. (1994) *Proc. Natl. Acad. Sci. U. S. A.* **91,** 1119–1123
67. Sheng, Z., Pennica, D., Wood, W. I., and Chien, K. R. (1996) *Development* **122,** 419–428
68. Bhatt, H., Brunet, L. J., and Steward, C. L. (1991) *Proc. Natl. Acad. Sci. U. S. A.* **88,** 11408–11412
69. Robertson, M., Chambers, I., Rathjen, P., Nichols, J., and Smith, A. (1993) *Dev. Genet.* **14,** 165–173

Cardiotrophin-1 Activates a Distinct Form of Cardiac Muscle Cell Hypertrophy: ASSEMBLY OF SARCOMERIC UNITS IN SERIES VIA gp130/LEUKEMIA INHIBITORY FACTOR RECEPTOR-DEPENDENT PATHWAYS

Kai C. Wollert, Tetsuya Taga, Mikiyoshi Saito, Masashi Narazaki, Tadamitsu Kishimoto, Christopher C. Glembotski, Ann B. Vernallis, John K. Heath, Diane Pennica, William I. Wood and Kenneth R. Chien

J. Biol. Chem. 1996, 271:9535-9545.
doi: 10.1074/jbc.271.16.9535
